The 5th European sCO2 Conference for Energy Systems
March 14-16, 2023, Prague, Czech Republic

2023-sCO2.eu-119

TECHNO-ECONOMIC ANALYSIS OF SCO2 POWER CYCLE FOR COAL-FIRED POWER SYSTEM

In Woo Son
Department of Nuclear and Quantum Engineering, Korea Advanced Institute of Science and Technology 373-1 Guseong-dong Yuseong-gu, Daejeon, 305-701, Korea
Email: siw4139@kaist.ac.kr

Jeong Ik Lee*
a Department of Nuclear and Quantum Engineering, Korea Advanced Institute of Science and Technology 373-1 Guseong-dong Yuseong-gu, Daejeon, 305-701, Korea
mail: jeongiklee@kaist.ac.kr

Yongju Jeong
Department of Nuclear and Quantum Engineering, Korea Advanced Institute of Science and Technology 373-1 Guseong-dong Yuseong-gu, Daejeon, 305-701, Korea
Email: jyjk7317@kaist.ac.kr

ABSTRACT

Supercritical CO_2 (sCO_2) power cycles are considered one of the promising candidates to replace a steam Rankine cycle. The sCO_2 power cycle has compact component size and minimum compression work because the supercritical state of CO_2 has a density similar to that of a liquid and a viscosity similar to that of a gas. Considering these advantages, many countries and institutions around the world are conducting research on the sCO_2 power cycle. However, most studies have focused on the thermal performance optimization of the power cycle, and an economic analysis and optimization is limited since experiences with sCO_2 power cycle commercial operation are not abundant. Fortunately, previous researchers have proposed expected component cost correlations for sCO_2 power cycle from cost data and literature survey [1]. In this paper, by utilizing the previously proposed component cost correlations, a sensitivity analysis of an sCO_2 power cycle with respect to the system's power output, cycle maximum temperature, fuel cost and cycle layout is conducted. From this study, a relation between the thermal performance optimization and the minimum cost is understood for the current technology level.

INTRODUCTION

The Supercritical Carbon dioxide (sCO_2) power cycle is a next-generation high-efficiency power cycle and is expected to be a candidate to replace the steam Rankine cycle [2]. Carbon dioxide is non-toxic, non-flammable, and has the critical point of 304.13K, 7.38 MPa, which is easily achievable.

Carbon dioxide in a supercritical state has a density similar to that of liquid and a viscosity similar to that of a gas at the same time. Therefore, the sCO_2 power cycle can have compact component size and minimum compression work, so it can be used in various energy sectors such as nuclear power, renewable energy, waste heat recovery, and marine propulsion [2]. Due to these advantages, the sCO_2 power cycle is being developed in many countries and institutions around the world, and pilot and demonstration plants are being constructed such as the STEP Demo pilot project [3], Sandia National Laboratories (SNL)'s test loop [4], sCO2 HeRO Loop [5], etc.

Studies on the sCO_2 power cycle are mainly focused on thermal performance evaluation, and relatively fewer studies on the economic analysis of the cycle are founded. This is because the current Technology Readiness Level (TRL) of the sCO_2 power cycle is 7 stages, so no commercial operation has been carried out [6]. The research on the economic analysis of the sCO_2 power cycle is an essential process before entering the TRL 8 and 9 stages which is the commercial operating stage.

* corresponding author(s)

DOI: 10.17185/duepublico/77279

Fig. 1 Roadmap phase for the sCO_2 power cycle of the SNL [6]

Nevertheless, some studies performed an economic analysis of the power cycle by developing cost models for the sCO_2 power cycle components [7-12]. However, few researches have studied the relationship between cost and performance for the sCO_2 power cycle rather than calculating the minimum power cycle cost [13, 14]. In the work of Benjelloun et al., a techno-economic analysis was performed on the direct and indirect recompression cycles and confirmed that both are suitable as a power cycle for next-generation nuclear power plants [13]. Alfani et al. performed techno-economic optimization of the sCO_2 power cycle integrated with CSP [14]. Among the four cycle layouts, they suggested that the recompression cycle with intercooling is the most promising from a perspective of the techno-economic and presented the optimal solution of the cycle.

In the previous studies, variables such as cycle component efficiency, pressure ratio and pinch temperature of a recuperator were set as parameters of sensitivity study [13, 14]. However, the power output and fuel cost for heat sources can also be set as parameters of the sensitivity study. This is because the power output affects the cost of cycle components, and the cycle performance determines the required fuel cost for electricity generation. Therefore, in this study, a techno-economic sensitivity study of the sCO_2 power cycle is performed with the power output and fuel cost. In addition, the previous studies have not examined whether a complex cycle is economically more effective compared to a simple recuperated cycle layout which is one of the simplest layouts [13, 14]. Therefore, in this study, a techno-economic analysis is aimed to observe whether the improvement in cycle performance due to the addition of components can be also economically beneficial.

To perform the economic analysis of the sCO_2 power cycle, data on the components' cost of the cycle are required. Fortunately, through cost data, literature surveys, and vendor quotes, the previous researchers have suggested the expected component cost of the sCO_2 power cycle concerning the component design [1]. The cost correlation for the cycle components is suggested and calculated for the total equipment cost of a 10MWe plant [15] and a 550MWe plant [16] as examples. In addition, the cost model has temperature correction factors to reflect the structural material change when the operating temperature is high.

$$f_T = \begin{cases} 1 & if\ T_{\max} < T_{bp} \\ 1 + c(T_{\max} - T_{bp}) + d(T_{\max} - T_{bp})^2 & if\ T_{max} \geq T_{bp} \end{cases} \quad (1)$$

In the previous studies, the temperature breakpoint of the temperature correction factor is set to 550°C, which the temperature is better to use a thinner nickel-based superalloy than the commonly used thicker stainless steel [1, 17]. Therefore, to consider this effect, the cycle maximum temperature is added as a parameter in the sensitivity study.

In this study, four variables are selected to be in total for the sensitivity study: cycle layout, cycle maximum temperature, fuel cost, and cycle power output, which significantly affect the Levelized Cost Of Energy (LCOE) of the sCO_2 power cycle and the corresponding cycle performance. The analysis of the sCO_2 power cycle is performed by using the component cost correlation of the sCO_2 power cycle suggested in the previous studies [1].

SCO_2 POWER CYCLE COST MODEL

In this study, the cycle thermal efficiency and the LCOE need to be calculated. To calculate these values, the sCO_2 power cycle design parameters should be set first. However, before setting the cycle design parameters, it is necessary to consider the cost model proposed in the previous study [1]. It is noted that this section will focus on the discussion of the application to Weiland's cost model presented in Ref. [1], since the major cost models utilized in this study is based on the Weiland's cost model.

From a material point of view, stainless steel is used for components operating below 550°C, and if not, nickel-based superalloy is used for higher temperatures components. This is incorporated to the cost model by using the high-temperature correction factor in equation (1) [1].

Weiland's research developed cost correlations for two types of primary heaters: natural gas-fired and coal-fired heaters [1]. These correlations include burners, fans, air preheaters, ductwork, headers, and connecting piping. In this study, the cost model for coal-fired heaters is used. This is because, the natural gas-fired heaters exist in the primary heater cost model of the previous study, but the valid range is too narrow (10 to 50 MW_{th}) [1] for this study. In this study, the heat source is limited to the coal-fired power field due to the limitation of the cost correlation equation of the primary heater in the previous study. However, in further study, the application areas can be expanded by using the cost correlations for other heat sources when more data is accumulated. The power range of the sCO_2 power cycle is set from 60MW_e to 500MW_e considering the valid range of the model for the coal-fired heaters.

As for the pre-cooler cost model, the direct air cooler type was provided in the previous study [1]. However, in this study, water/sCO_2 PCHE is used for the pre-cooler. Fortunately, in the previous study, the recuperator cost model can be used conservatively for water/sCO_2 PCHE pre-cooler [1]. Therefore,

DOI: 10.17185/duepublico/77279

in this study, the cost model for the recuperator is used for the cost model of the pre-cooler.

The model selection of compressors and motors is more complicated than other components. In the previous study, the compressor cost model consists of integrally geared (IG) centrifugal type and barrel-type centrifugal compressors [1]. For the cost model of motor, three types are suggested in the previous study [1]: explosion-proof motors (EPM), synchronous motors (SM), and open drop-proof motors (OM). The cost model of each motor is as follows. The EPM cost model has the lowest cost and that of the OM has the highest cost. Therefore, it is necessary to subdivide the motor for the required compressor work. For the recompression cycle layout, since the main compressor and re-compressor exist, it is necessary to consider whether the shaft is separated or single. The maximum valid range of the motor cost model is $37MW_e$, so if the combined work of the main compressor and re-compressor is less than $37MW_e$, it can be operated with one motor. However, if not, the shaft of the compressor must be separated and operated with each motor.

If the work of one compressor exceeds the maximum motor model range of 37MWe, additional calculation is required. In the previous study, the calculations were performed using multiple barrel-type compressors and assuming each fitted with a motor [1]. Therefore, in this study, when one compressor work exceeds $37MW_e$, a multiple barrel-type compressor is used by dividing the compressors' work. To comply with the limits of the valid range of the cost models for motors and compressors, the divided compressor work is less than $37MW_e$ and the divided compressor volumetric flowrate is less than $2.4\ m^3/s$. The detailed compressor and motor cost calculation process is as follows.

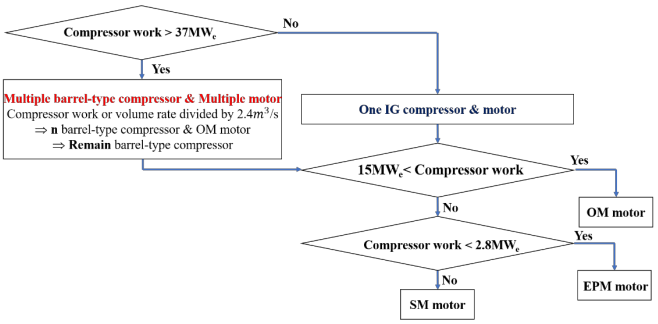

Fig. 2 Compressor and motor cost model selection algorithm

Therefore, the purchased equipment cost (PEC) of the sCO_2 power cycle can be calculated as follows. The process for obtaining the LCOE is covered in detail in the LCOE calculation section.

$$PEC = C_{PHX} + C_{Recup} + C_{Turb} + C_{Comp} + C_{Motor} + C_{Generator} \quad (2)$$

SCO_2 POWER CYCLE OPTIMIZATION

The cost models are summarized in Table 1. Three cycle power outputs within the valid range of cost models are set as shown. Therefore, a fair comparison of the power cycle could be made within the valid range of the cost model. In addition, to study the effect of the temperature correction factor in the cost model, two different maximum cycle temperature was reviewed: 550 and 650 °C. Other parameters are set as shown in Table 1 based on the references [18, 19]. Two different sCO_2 power cycle layouts are selected for comparison: simple recuperated cycle layout and recompression cycle layout as shown in Fig 3 and 4, respectively.

Table 1. Cycle design parameters and optimization variables

Maximum Temperature (°C)	550, 650
Cycle output (MW_e)	60, 100, 500
Maximum pressure (MPa)	25
Minimum temperature (°C)	35
Turbine efficiency (%)	85
Compressor efficiency (%)	80
Component pressure drop (Kpa)	100-150
HTR, LTR effectiveness (%)	90
Generator efficiency (%)	98
Optimization variables	
Pressure ratio (2.62~3.24 for simple recuperated cycle) (2.49~3.05 for recompression cycle)	
Flow split ratio (0.5~0.99 for recompression cycle layout)	

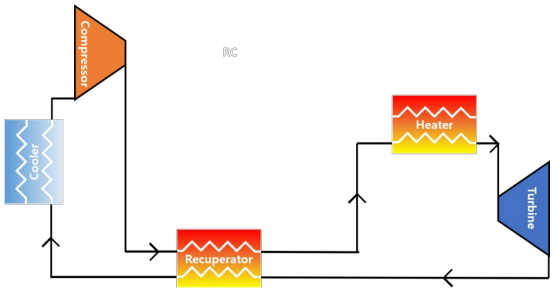

Fig. 3 simple recuperated cycle layout

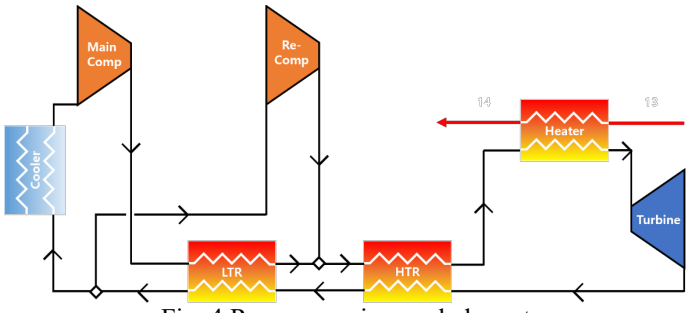

Fig. 4 Recompression cycle layout

Therefore, cycle optimization is performed using the KAIST-CCD code. The KAIST-CCD code is a MATLAB-based in-house code and has been developed by the KAIST research

DOI: 10.17185/duepublico/77279

team. The physical properties of the sCO_2 are calculated with NIST-REFPROP database for accurate calculation of properties [20]. The operation algorithm of the KAIST-CCD code is shown in Figure 5, and the error of the algorithm is as follows.

$$\text{Error} = \frac{[\text{heat input(n)} - \text{heat input(n-1)}]}{\text{heat input(n)}} \quad (3)$$

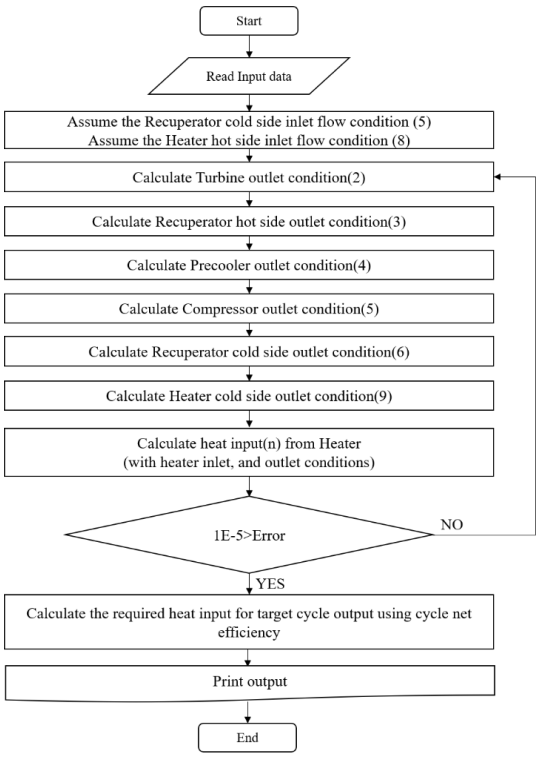

Fig. 5 Operation algorithm of the KAIST-CCD code

The optimization results for each cycle maximum temperature, output, and layout are summarized in Tables 2 and 3, and the cycle optimization results are shown in Fig 6,7 and 8. Fig. 6 (a) is the pressure ratio-efficiency graph for the cycle maximum temperature of 550°C, and Fig. 6 (b) is the same graph for the cycle maximum temperature of 650°C. For the recompression cycle, the optimization variables are the pressure ratio and flow split ratio. Fig. 7 shows the optimization result graph for the maximum cycle temperature of 550°C, and Fig. 8 shows the graph for the maximum cycle temperature of 650°C.

Table 2. Cycle optimization results for simple recuperated cycle

Cycle maximum temperature (°C)	550	650
Cycle thermal efficiency (%)	31.85	34.47
Cycle output (MW_e)	60 / 100 / 500	60 / 100 / 500
Required thermal power (MW_{th})	188 / 314 / 1570	174 / 290 / 1450
Pressure ratio	2.97	2.97

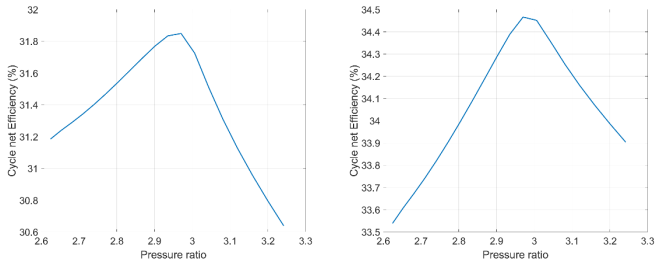

Fig. 6 Cycle optimization results for simple recuperated cycle by cycle maximum temperature (a) 550°C (b) 650°C

Table 3. Cycle optimization results for recompression cycle

Cycle maximum temperature (°C)	550	650
Cycle thermal efficiency (%)	38.17	41.80
Cycle output (MW_e)	60 / 100 / 500	60 / 100 / 500
Required thermal power (MW_{th})	157 / 262 / 1310	144 / 239 / 1196
Pressure ratio	2.74	2.81
Flow split ratio	0.7	0.7

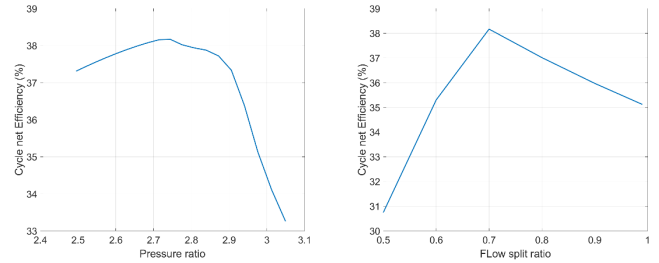

Fig. 7. Cycle optimization results for recompression cycle for cycle maximum temperature 550°C (a) Pressure ratio-Efficiency (b) Flow split ratio-Efficiency

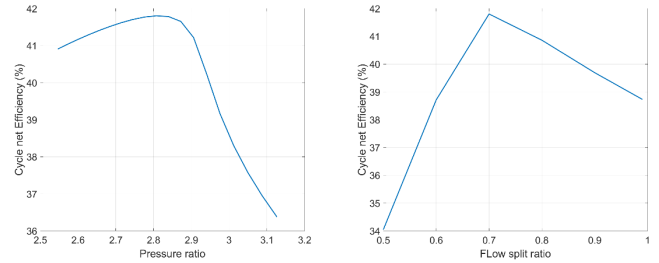

Fig. 8 Cycle optimization results for recompression cycle for cycle maximum temperature 650°C (a) Pressure ratio-Efficiency (b) Flow split ratio-Efficiency

DOI: 10.17185/duepublico/77279

RECUPERATOR AND PRE-COOLER CONDUCTANCE-AREA CALCULATION

To utilize the cost model of the recuperator and pre-cooler, the conductance-area product, UA, of each heat exchanger should be calculated. The cycle design points within the optimization range are obtained by performing cycle optimization. Therefore, the conductance-area product UA can be calculated using the heat exchanger inlet and outlet temperatures and pressures. In the previous study, as a result of calculating UA through the discretized heat exchanger model using the REFPROP database [20], precise calculations can be performed even with 20 nodes [1]. Therefore, in this study, a discretized heat exchanger model with 200 nodes is developed to accurately calculate UA. This code uses the NIST REFPROP database [20], and the conductance-area product UA of each node can be calculated through the following LMTD method using the inlet and outlet temperature of the heat exchanger. Therefore, the UA of the heat exchanger can be calculated.

$$\dot{Q}_{Re}(W) = UA_{\text{heat transfer}}\Delta T_m \quad (4)$$

$$\Delta T_m = \frac{(T_{\text{hot in}} - T_{\text{cold out}}) - (T_{\text{hot out}} - T_{\text{cold in}})}{\ln((T_{\text{hot in}} - T_{\text{cold out}})) - \ln((T_{\text{hot out}} - T_{\text{cold in}}))} \quad (5)$$

Since it is difficult to show the UA at the all design point within optimization variables, only the UA at the cycle optimum point is shown in Table 4 and 5. The UA of the recuperator and pre-cooler at the optimal point for each cycle layout are as follows.

Table 4. UA calculation results for simple recuperated cycle layout

Cycle maximum temperature (°C)	550	650
Cycle output (MW_e)	60 / 100 / 500	60 / 100 / 500
Required thermal power (MW_{th})	188 / 314 / 1570	174 / 290 / 1450
Recuperator UA (MW/K)	3.1 / 5.2 / 25.8	2.7 / 4.4 / 22.3
Pre-cooler UA (MW/K)	12.6 / 21.1 / 105.4	10.8 /18.0 / 89.8

Table 5. UA calculation results for recompression cycle layout

Cycle maximum temperature (°C)	550	650
Cycle output (MW_e)	60 / 100 / 500	60 / 100 / 500
Required thermal power (MW_{th})	157 / 262 / 1310	144 / 239 / 1196
Hot Temp Recuperator UA (MW/K)	4.8 / 8.0 / 40.2	4.3 / 7.2 / 35.9
Low Temp Recuperator UA (MW/K)	7.8 / 13.0 / 65.2	5.4 / 9.0 / 44.9
Pre-cooler UA (MW/K)	19.2 / 31.7 / 158.5	16.8 / 27.9 / 139.7

LCOE CALCULATION

The Levelized Cost Of Energy (LCOE) is a measure of the average net present cost of electricity production over the lifetime of a power plant. The LCOE is defined with the following equation (17). In the equation, I_t is the Fixed Capital Cost (FCI), M_t is the Operation and Maintenance (O&M, M_t) costs, F_t is the fuel expenditures in year t, E_t is the electricity energy generated in the year t, r is the discount rate, and t is the expected life time. The load factor used in this study is 53.5%, which is the load factor of coal-fired power plants worldwide in 2019 [21].

$$LCOE = \frac{\sum_{t=1}^{n}\left[\frac{I_t + M_t + F_t}{(1+r)^t}\right]}{\sum_{t=1}^{n}\frac{E_t}{(1+r)^t}} \quad (6)$$

According to references, FCI consists of direct cost (DC) and indirect cost (IC), and O&M cost is a cost related to FCI [21]. The direct cost refers to the cost that directly affects the system, such as structural, piping, and civil costs. Indirect cost means the cost that is indirectly related to the system, such as contingency, supervision, and engineering. The DC is the cost associated with the purchased equipment cost (PEC) in equation (13), and IC is the cost affected by DC [22]. The purchased equipment installation cost for each component referred to Weiland's research [1]. The piping cost is 20% of the PEC when the maximum cycle temperature exceeds 550°C, and 5% of the PEC otherwise [1]. Therefore, direct cost, indirect cost, and operating maintenance cost are summarized in Table 6 [1, 22].

$$I_t = FCI\ (Fixed\ Capital\ Cost) = DC + IC \quad (7)$$

$$M_t = O\&M = function(FCI)_{Table\ 6} \quad (8)$$

$$DC\ (Direct\ Cost) = function(PEC)_{Table\ 6} \quad (9)$$

$$IC\ (Indirect\ Cost) = function(DC)_{Table\ 6} \quad (10)$$

Table 6 O&M, IC, DC cost [1, 22]

O&M cost (M_t)	
Fixed operating and maintenance	6.8% of FCI
Various operating and maintenance	6.1% of Fixed O&M

DOI: 10.17185/duepublico/77279

Indirect Cost (IC)	
Engineering and supervision	8% of DC
Construction cost and contractor's profit	15% of DC
Contingency	15% of DC
Direct Cost (DC)	
Purchased equipment installation [1]	50% of PEC [Primary heat exchanger] 20% of PEC [Other components] 5% of PEC [Recuperator]
Piping [1]	5% of PEC ($T_{max} < 550°C$) 20% of PEC ($T_{max} > 550°C$)
Instrumentation & controls	10% of PEC
Civil, structural, and architectural factor	30% of PEC
Service facilities	30% of PEC

In this study, the fuel is coal. The cost of coal is referred a trading site [23]. since the fuel price is used as a variable in the sensitivity analysis, the lowest and the highest fuel costs for one year are used for 1st August 2022.

Table 7. Fuel cost of the sCO_2 power cycle

Fuel cost (F_t) [23]		
Fuel (Coal)	18.4~51.6	$/MWh$_{th}$

SENSITIVITY STUDY

The relation between the optimum cycle thermal efficiency and the LCOE minimum point is investigated with a sensitivity analysis in this study. Table 8 shows the range of variables for sensitivity analysis. The discount rate and lifetime of the sCO_2 power cycle required for LCOE calculation are set to 5% [24-26] and 40 years [27, 28], respectively.

Table 8. The variable range used for sensitivity analysis

Cycle output (MW_e)	6-500
Cycle Maximum Temperature, T_{max} (°C)	550-650
Fuel (Coal) cost ($/$MWh_{th}$)	18.4-51.6
Cycle layout	Simple recuperated cycle Recompression cycle

CASE 1: SIMPLE RECUPERATED CYCLE (T_{max} = 550°C)

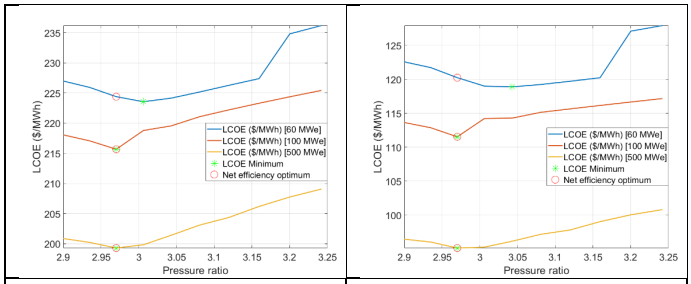

(a) Fuel cost = high (b) Fuel cost = low

Fig. 9 sCO_2 power cycle LCOE results for pressure ratio and fuel cost (T_{max} =550°C, Cycle output = 60, 100, 500MW_e)

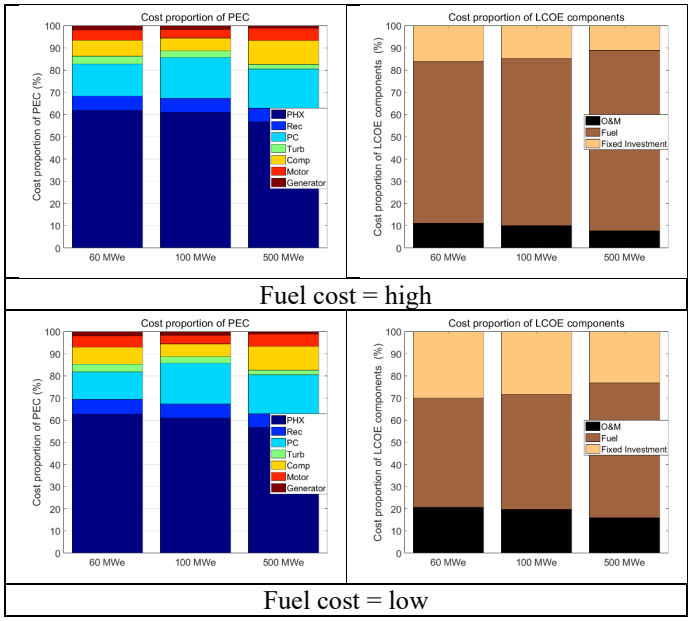

Fuel cost = high

Fuel cost = low

Fig. 10 PEC (a) and LCOE (b) of the sCO_2 power cycle (T_{max} = 550°C, Cycle output = 60, 100, 500MW_e)

The results for each fuel cost and cycle output are shown for a simple recuperated cycle layout with a cycle maximum temperature of 550°C. The larger the cycle output, the closer the cycle thermal performance optimum point and the LCOE minimum point is. This is because the component costs take the form of a function of cost = x^n (n<1), so the cost converges as the output of the system increases. Therefore, the percentage of fixed investment cost which related to the component cost decreases as the cycle output increases as shown in Fig. 10. In other words, as the cycle output increases, the fixed investment

DOI: 10.17185/duepublico/77279

cost converges to a certain value. On contrary, as the cycle output increases, the cost of fuel increases linearly. These results suggest that the fuel costs have a significant impact on LCOE when the cycle output is large enough. Therefore, the LCOE minimum point with large the cycle output approaches the optimum point of cycle thermal efficiency requiring the least additional heat sources.

The LCOE decreases as the system output increases as shown in Fig. 9. However, due to the limitation on the valid range of the compressor and motor cost models; it is necessary to use multiple compressors and motors. Therefore, it can be seen that the LCOE for the pressure ratio increases stepwise depending on whether multiple compressors and motors are used. As can be seen from the bar graph for percentage change in component cost in PEC, as the system output increases, unlike other components, the cost fraction of compressor as well as motor increases.

When the fuel cost is low, LCOE decreases. The percentage of fuel in LCOE shows a large difference such that about 22% decreases compared to that of the high fuel cost case. As fuel cost decreases, the cost for additional heat sources required at non-optimal cycle efficiencies decreases. This effect smooths the slope of the LCOE with respect to the pressure ratio.

CASE 2: SIMPLE RECUPERATED CYCLE (T_{max} = 650°C)

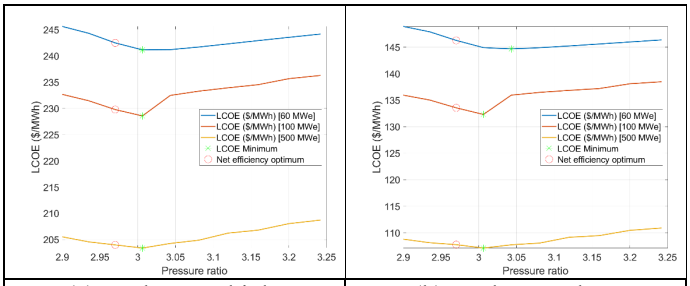

(a) Fuel cost = high | (b) Fuel cost = low

Fig. 11 sCO_2 power cycle LCOE results for pressure ratio and fuel cost (T_{max} = 650°C, Cycle output = 60, 100, 500MW_e)

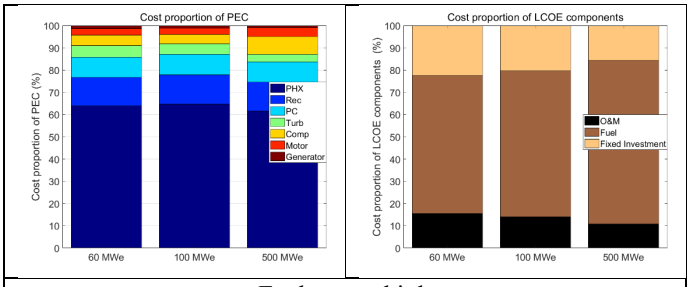

Fuel cost = high

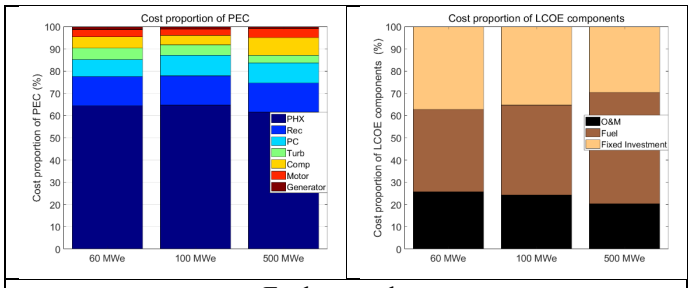

Fuel cost = low

Fig. 12 PEC (a) and LCOE (b) of the sCO_2 power cycle (T_{max} = 650°C, Cycle output = 500MW_e)

For the cycle maximum temperature 650°C case, the costs of high-temperature components, such as primary heater, turbine, and recuperator, increase due to the temperature correction factor. As shown in Fig. 12 (a), the fraction of primary heater, turbine, and recuperator increases compared to the case with 550°C.

As shown in Fig.12 (b), it is confirmed that the fraction of the fixed investment cost related to the component cost increases. Therefore, the effect of fuel cost on the LCOE is reduced compared to that of 550°C case, and this effect can be confirmed with the fact that the cycle efficiency optimum point and the minimum LCOE point do not match with each other, which is in contrast with the 550°C result.

If the fuel cost is low, the LCOE decreases, and the fraction of fuel in the LCOE is reduced by 24%. The fuel cost affects the cost of the additional heat required to produce the same cycle power output with the lower cycle efficiency cases. Therefore, when the fuel cost is low, the effect of the cycle optimum efficiency on the LCOE becomes small. This effect confirmed that the cycle optimum point and the LCOE minimum point do not match in the case of a low fuel cost as shown in Fig. 11.

CASE 3: RECOMPRESSION CYCLE (T_{max} = 550°C)

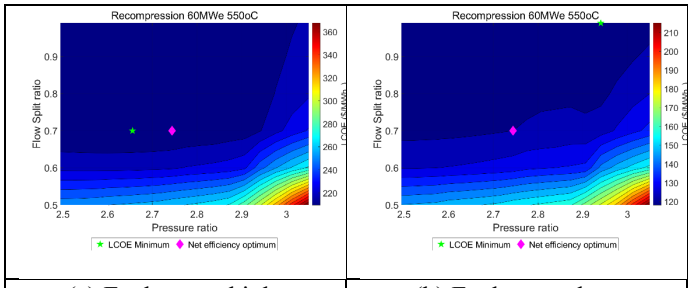

(a) Fuel cost = high | (b) Fuel cost = low

Fig. 13 sCO_2 power cycle LCOE results for pressure ratio and fuel cost (T_{max} = 550°C, Cycle output = 60MW_e)

DOI: 10.17185/duepublico/77279

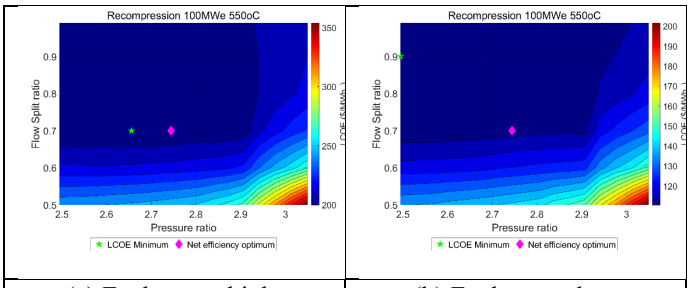

(a) Fuel cost = high | (b) Fuel cost = low

Fig. 14 sCO_2 power cycle LCOE results for pressure ratio and fuel cost ($\mathbf{T_{max}}$ = 550°C, Cycle output = 100MW_e)

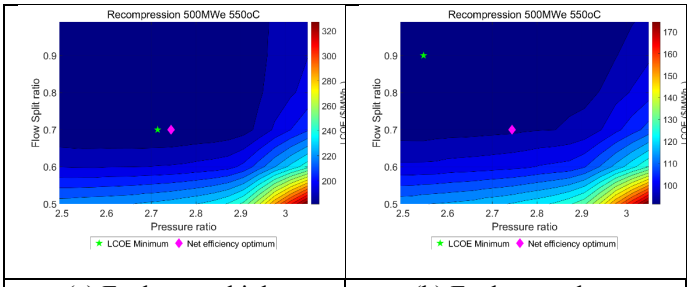

(a) Fuel cost = high | (b) Fuel cost = low

Fig. 15 sCO_2 power cycle LCOE results for pressure ratio and fuel cost ($\mathbf{T_{max}}$ = 550°C, Cycle output = 500MW_e)

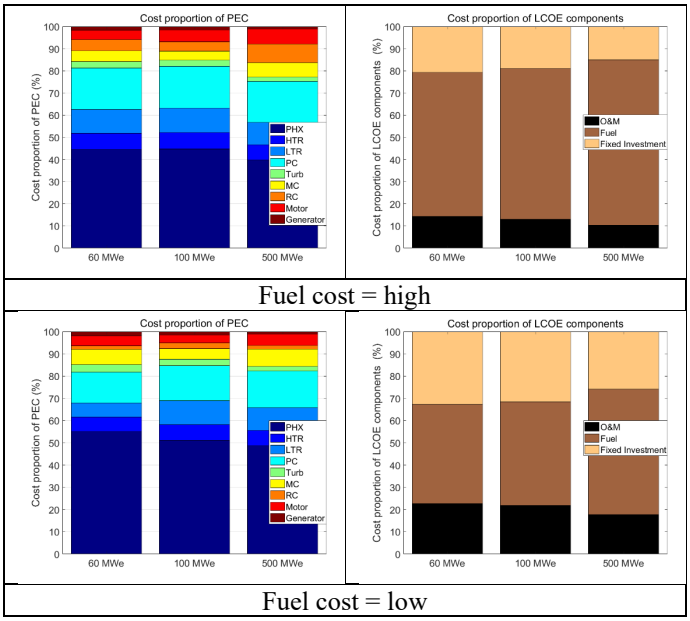

Fuel cost = high

Fuel cost = low

Fig. 16 PEC (a) and LCOE (b) of the sCO_2 power cycle ($\mathbf{T_{max}}$ = 550°C, Cycle output = 60,100, 500MW_e)

The recompression cycle improves the cycle efficiency by adding recompressing process. In this cycle, heat rejection can be reduced by splitting the mass flow rate before the pre-cooler as shown in Fig. 4. Compared to the simple recuperated cycle layout, the recompression cycle has more components. Therefore, the fraction of fixed investment cost in LCOE increases compared to the simple recuperated cycle layout.

When the cycle output and fuel cost is small, the increase in component cost is larger than the increase in work due to the recompression effects, resulting in higher LCOE compared to that of the simple recuperated cycle. Therefore, the minimum LCOE occurred in the direction of the simple recuperated cycle (FSR = 100%) at low power output (60, 100MW_e) and low fuel cost as shown in Fig. 13(b). Conversely, if the cycle output is larger than 100MW_e, the component cost does not significantly affect the LCOE. This is because the component cost function has the form x^n (n<1). In other words, when the system output is large enough, the minimum LCOE point converges to a cycle optimal point with the lowest fuel cost. Therefore, it is confirmed that the larger the system output and the higher the fuel cost are, the greater the effect of recompression becomes.

The fraction of fuel cost in LCOE decreases by 20% when the fuel cost decreases as shown in Fig.16. This result shows that the fraction of the fuel cost in LCOE is reduced, so that the LCOE is more sensitive to the cycle component cost. Therefore, the lowest point of the LCOE is not closer to the optimum cycle efficiency point compared to when the fuel cost is high.

CASE 4: RECOMPRESSION CYCLE ($\mathbf{T_{max}}$ =650°C)

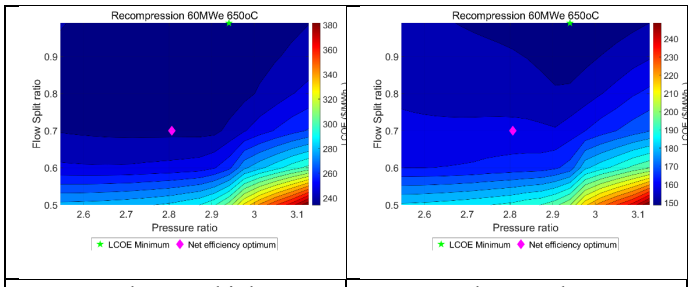

Fuel cost = high | Fuel cost = low

Fig. 17 sCO_2 power cycle LCOE results for pressure ratio and fuel cost ($\mathbf{T_{max}}$ = 650°C, Cycle output = 60MW_e)

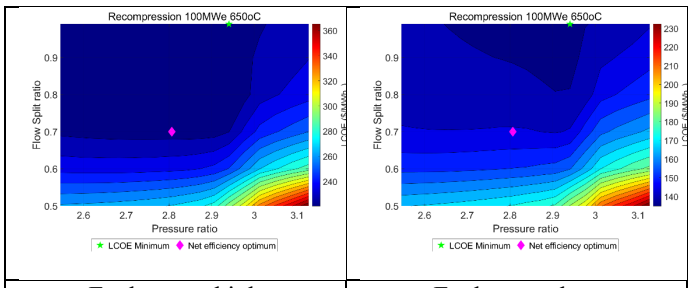

Fuel cost = high | Fuel cost = low

Fig. 18 sCO_2 power cycle LCOE results for pressure ratio and fuel cost ($\mathbf{T_{max}}$ = 650°C, Cycle output = 100MW_e)

DOI: 10.17185/duepublico/77279

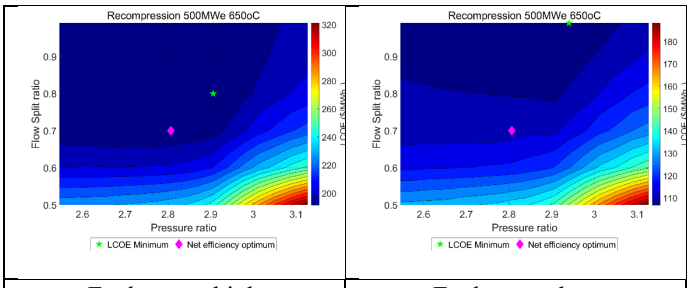

Fuel cost = high | Fuel cost = low

Fig. 19 sCO_2 power cycle LCOE results for pressure ratio and fuel cost ($\mathbf{T_{max}}$ = 650°C, Cycle output = 500MW_e)

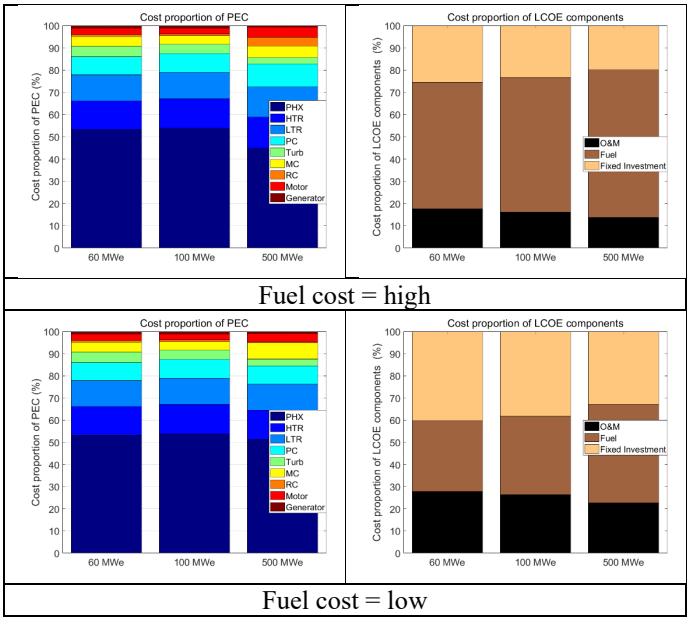

Fuel cost = high

Fuel cost = low

Fig. 20 PEC and LCOE of the sCO_2 power cycle ($\mathbf{T_{max}}$ = 650°C, Cycle output = 60, 100, 500MW_e)

In the case of 650°C case, the cost and the cost escalation of high-temperature components increase due to the temperature correction factor. Therefore, the effect of fixed investment costs on LCOE increases as shown in Fig. 20 (b).

When the fuel cost is low, component costs have a significant impact on LCOE. Therefore, the effect of recompression is hardly seen in the case of low fuel cost and 650°C as shown in Figs. 17, 18, 19.

SUMMARY AND CONCLUSIONS

In this study, techno-economic sensitivity analysis is performed on the correlation between the LCOE minimum point and the optimum cycle performance for the sCO_2 power cycle.

The correlation between the best cycle performance and the lowest LCOE point is determined by the impact of the following key variables on fixed investment costs and fuel costs: 1. Cycle power output, 2. Cycle maximum temperature, 3. Fuel cost, 4. Cycle layout. The sensitivity analysis for cycle performance and LCOE is performed for these four factors.

First, it is confirmed that the LCOE minimum point converges to the optimum point of cycle efficiency as the cycle power output increases. This is because, as the cycle power output increases, the cost of the cycle component converges, while the cost of the required fuel increases proportionally to the cycle power output.

Second, as the maximum cycle temperature exceeds 550°C, the cost of the component increases due to the temperature correction factor. As the maximum cycle temperature increases (over 550°C), the fraction of fixed investment costs in the LCOE increases, so the LCOE minimum point becomes distant from the cycle efficiency optimum point.

Third, as the fuel cost increases, the fraction of fuel cost in LCOE increases. As the cycle efficiency approaches the optimum efficiency, the fuel required to generate the same cycle power output decreases. Therefore, the higher the fuel cost is, the greater the effect of cycle efficiency on LCOE is. Therefore, as the fuel cost increases, it is confirmed that the cycle efficiency optimum point and the LCOE minimum point are close.

Finally, as a result of comparing the cycle layout, it is confirmed that the recompression effect increases as the system output and the fuel cost increases. That is, a sufficiently large power cycle output or a high fuel cost for a heat source is required to benefit from the addition of a recompression process. However, in the current level of technology, the thermal performance optimum and the LCOE minimum of the recompression cycle do not match with each other under ranges of variables considered in this study.

In conclusion, it is confirmed that the cycle best performance and the minimum LCOE points generally do not coincide as the cycle becomes more complex and the cycle maximum temperature becomes high. The discrepancy between the cycle performance and the LCOE shows that cycle design optimization should consider not only the cycle performance, but also the economic performance as well at the current technology level. When the cost data is more accumulated after the sCO_2 power cycle enters higher technology readiness level in the future, it can be expected that the cost model will be improved even at higher temperatures and smaller sizes. As the proposed future study, the techno-economical sensitivity of the sCO_2 power cycle will be performed for considering wider range of variables, such as recuperator conductance-area product UA, updated material costs, pipe costs and, discount rate, etc [9].

NOMENCLATURE

ΔT_m	Log mean temperature
C	Component cost
F_t	Fuel expenditures in year t
f_T	Temperature correction factor
I_t	Fixed capital cost in year t
M_t	Operation and maintenance cost in year t

DOI: 10.17185/duepublico/77279

r	Discount rate
T	Temperature
t	Power cycle life time
T_{max}	Cycle maximum temperature
UA	Conductance-area product

ACKNOWLEDGEMENTS

This research was supported by Civil-Military Technology Cooperation Program (iCMTC) funded by the Agency for Defense Development – South Korea (17-CM-EN-04).

REFERENCES

[1] Weiland, Nathan T., Blake W. Lance, and Sandeep R. Pidaparti. "SCO2 power cycle component cost correlations from DOE data spanning multiple scales and applications." Turbo Expo: Power for Land, Sea, and Air. Vol. 58721. American Society of Mechanical Engineers, 2019.

[2] Ahn, Yoonhan, et al. "Review of supercritical CO2 power cycle technology and current status of research and development." Nuclear engineering and technology 47.6 (2015): 647-661.

[3] Marion, John, et al. "The STEP 10 MWe sCO2 Pilot Demonstration Status Update." Turbo Expo: Power for Land, Sea, and Air. Vol. 86083. American Society of Mechanical Engineers, 2022.

[4] Pasch, James Jay, et al. Supercritical CO2 recompression Brayton cycle: completed assembly description. No. SAND2012-9546. Sandia National Laboratories (SNL), Albuquerque, NM, and Livermore, CA (United States), 2012.

[5] Hacks, Alexander Johannes, et al. "Operational experiences and design of the sCO2-HeRo loop." 3rd European supercritical CO2 Conference. 2019.

[6] Mendez Cruz, Carmen Margarita, and Gary E. Rochau. sCO2 Brayton Cycle: Roadmap to sCO2 Power Cycles NE Commercial Applications. No. SAND-2018-6187. Sandia National Lab.(SNL-NM), Albuquerque, NM (United States), 2018.

[7] Wright, Steven A., Chal S. Davidson, and William O. Scammell. "Thermo-economic analysis of four sCO2 waste heat recovery power systems." Fifth International SCO2 Symposium, San Antonio, TX, Mar. 2016.

[8] Meybodi, Mehdi Aghaei, et al. "Techno-economic analysis of supercritical carbon dioxide power blocks." *AIP Conference Proceedings*. Vol. 1850. No. 1. AIP Publishing LLC, 2017.

[9] Neises, Ty, and Craig Turchi. "Supercritical carbon dioxide power cycle design and configuration optimization to minimize levelized cost of energy of molten salt power towers operating at 650 C." *Solar Energy* 181 (2019): 27-36.

[10] Thanganadar, Dhinesh, et al. "Techno-economic analysis of supercritical carbon dioxide cycle integrated with coal-fired power plant." *Energy Conversion and Management* 242 (2021): 114294.

[11] Marchionni, Matteo, et al. "Techno-economic comparison of different cycle architectures for high temperature waste heat to power conversion systems using CO2 in supercritical phase." *Energy Procedia* 123 (2017): 305-312.

[12] Wang, Xurong, and Yiping Dai. "Exergoeconomic analysis of utilizing the transcritical CO2 cycle and the ORC for a recompression supercritical CO2 cycle waste heat recovery: A comparative study." *Applied energy* 170 (2016): 193-207.

[13] Benjelloun, M., G. Doulgeris, and R. Singh. "A method for techno-economic analysis of supercritical carbon dioxide cycles for new generation nuclear power plants." Proceedings of the Institution of Mechanical Engineers, Part A: Journal of Power and Energy 226.3 (2012): 372-383.

[14] Alfani, Dario, et al. "Techno-economic analysis of CSP incorporating sCO2 brayton power cycles: Trade-off between cost and performance." AIP Conference Proceedings. Vol. 2445. No. 1. AIP Publishing LLC, 2022.

[15] White, Charles W., et al. Techno-economic Evaluation of Utility-Scale Power Plants Based on the Indirect sCO2 Brayton Cycle-Report. No. 21490. National Energy Technology Laboratory (NETL), Pittsburgh, PA, Morgantown, WV (United States), 2017.

[16] Zitney, Stephen E., and Eric Liese. Dynamic Modeling and Simulation of a 10MWe Supercritical CO2 Recompression Closed Brayton Power Cycle for Off-Design, Part-Load, and Control Analysis. No. NETL-PUB-21414. National Energy Technology Laboratory (NETL), Pittsburgh, PA, Morgantown, WV (United States), 2017.

[17] Mecheri, Mounir. "SCO2 closed Brayton cycle for coal-fired power plant: An economic analysis of a technical optimization." 2nd European sCO2 Conference 2018: 30-31 August 2018, Essen, Germany. 2018.

[18] SunShot Vision Study. N.p.: U.S. Department of Energy, Feb. 2012. PDF.

[19] Le Moullec, Yann, et al. "Shouhang-EDF 10MWe supercritical CO2 cycle+ CSP demonstration project." 3rd European Conference on Supercritical CO2 (sCO2) Power Systems 2019: 19th-20th September 2019.

[20] E.W. Lemmon, M.L. Huber, and M. O. McLinden, "NIST Standard Reference Database 23," NIST Reference Fluid Thermodynamic and Transport Properties –REFPROP, version, vol.9, p.55, 2010.

[21] "Carbonbrief", CabonBrief.org, last modified March 26, 2020, accessed December 27. 2022, https://www.carbonbrief.org/mapped-worlds-coal-power-plants/

[22] Bejan, Adrian, George Tsatsaronis, and Michael J. Moran. Thermal design and optimization. John Wiley & Sons, 1995.

[23] "TRADING ECONOMICS", TRADING ECONOMICS, last modified August 1. 2022, accessed August 1. 2022, https://tradingeconomics.com/commodity/coal

[24] Arrow K, Cropper M, Gollier C, Groom B, Heal G, Newell R, et al. Determining benefits and costs for future generations. Science 2013;341:349–50.

[25] Locatelli G, Boarin S, Fiordaliso A, Ricotti ME. Load following of Small Modular Reactors (SMR) by cogeneration of hydrogen: a techno-economic analysis. Energy 2018;148:494–505.

[26] Rath Michael, Granger Morgan M. Assessment of a hybrid system that uses small modular reactors (SMRs) to back up intermittent renewables and desalinate water. Prog Nucl Energy 2020;122:103269.

[27] Bundesnetzagentur. Power plant list. 2019. https://www.undesnetzagentur.de/EN/Areas/Energy/Companies/SecurityOfSupply/GeneratingCapacity/PowerPlantList/PubliPowerPlantList_node.html. Accessed March 14, 2019.

[28] Fiebrandt, Marc, Julian Röder, and Hermann-Josef Wagner. "Minimum loads of coal-fired power plants and the potential suitability for energy storage using the example of Germany." International Journal of Energy Research 46.4 (2022): 4975-4993.

DOI: 10.17185/duepublico/77279

DOI: 10.17185/duepublico/77279
URN: urn:nbn:de:hbz:465-20230427-114558-7